JCI The Journal of Clinical Investigation

Methyldopa blocks MHC class II binding to disease-specific antigens in autoimmune diabetes

David A. Ostrov, … , Peter A. Gottlieb, Aaron W. Michels

J Clin Invest. 2018. https://doi.org/10.1172/JCI97739.

Research Article In-Press Preview **Autoimmunity** **Endocrinology**

Major histocompatibility (MHC) class II molecules are strongly associated with many autoimmune disorders. In type 1 diabetes, the DQ8 molecule is common, confers significant disease risk and is involved in disease pathogenesis. We hypothesized blocking DQ8 antigen presentation would provide therapeutic benefit by preventing recognition of self-peptides by pathogenic T cells. We used the crystal structure of DQ8 to select drug-like small molecules predicted to bind structural pockets in the MHC antigen-binding cleft. A limited number of the predicted compounds inhibited DQ8 antigen presentation in vitro with one compound preventing insulin autoantibody production and delaying diabetes onset in an animal model of spontaneous autoimmune diabetes. An existing drug of similar structure, methyldopa, specifically blocked DQ8 in recent-onset patients with type 1 diabetes along with reducing inflammatory T cell responses toward insulin, highlighting the relevance of blocking disease-specific MHC class II antigen presentation to treat autoimmunity.

Methyldopa blocks MHC class II binding to disease-specific antigens in autoimmune diabetes

David A. Ostrov[1], Aimon Alkanani[2], Kristen A. McDaniel[2], Stephanie Case[2], Erin E. Baschal[2], Laura Pyle[2,3], Sam Ellis[2,4], Bernadette Pöllinger[5], Katherine J. Seidl[5], Viral N. Shah[2], Satish K. Garg[2], Mark A. Atkinson[1], Peter A. Gottlieb[2,6], Aaron W. Michels[2,6*]

[1]Department of Pathology, Immunology, and Laboratory Medicine, College of Medicine, University of Florida, Gainesville, FL, USA

[2]Barbara Davis Center for Childhood Diabetes, University of Colorado School of Medicine, Aurora, CO, USA

[3]Department of Biostatistics and Informatics, University of Colorado School of Public Health Aurora, CO, USA

[4]Department of Clinical Pharmacy, University of Colorado, Aurora, CO, USA

[5]Novartis Institutes for Biomedical Research, 4002 Basel, Switzerland

[6]These authors contributed equally to this work.

[*]Corresponding Author

Aaron Michels, M.D.

Barbara Davis Center for Childhood Diabetes

University of Colorado School of Medicine

1775 Aurora Court A-140

Aurora, CO 80045

303-724-1923

Aaron.michels@ucdenver.edu

Conflict of Interest Statement

A.W. Michels and D.A. Ostrov are inventors on a patent, Compounds That Modulate Autoimmunity and Methods of Using the Same, licensed to ImmunoMolecular Therapeutics. A.W. Michels and P.A. Gottlieb are scientific cofounders of ImmunoMolecular Therapeutics and own shares in the company. K.J. Siedl and B. Pollinger were employees at Novartis and may own Novartis stock.

ABSTRACT

Major histocompatibility (MHC) class II molecules are strongly associated with many autoimmune disorders. In type 1 diabetes, the DQ8 molecule is common, confers significant disease risk and is involved in disease pathogenesis. We hypothesized blocking DQ8 antigen presentation would provide therapeutic benefit by preventing recognition of self-peptides by pathogenic T-cells. We used the crystal structure of DQ8 to select drug-like small molecules predicted to bind structural pockets in the MHC antigen-binding cleft. A limited number of the predicted compounds inhibited DQ8 antigen presentation in vitro with one compound preventing insulin autoantibody production and delaying diabetes onset in an animal model of spontaneous autoimmune diabetes. An existing drug of similar structure, methyldopa, specifically blocked DQ8 in recent-onset patients with type 1 diabetes along with reducing inflammatory T-cell responses toward insulin, highlighting the relevance of blocking disease-specific MHC class II antigen presentation to treat autoimmunity.

INTRODUCTION

Type 1 diabetes (T1D) results from the chronic autoimmune mediated destruction of insulin producing beta cells within pancreatic islets (1, 2). There is a wealth of knowledge regarding disease pathogenesis and natural history such that T1D is predictable by assessment of serum islet autoantibodies years prior to symptom onset (3). With a predictable nature and increasing incidence (4), a number of immune therapies have been tested in well-controlled clinical trials seeking to prevent or slow the loss of beta cell decline, including therapies targeted to CD2 or CD3 on T-cells (5-8), CD20 on B-cells (9), CD80/86 on antigen presenting cells (APCs) (10), inflammatory cytokines (IL-1 and IL-1 receptor) (11) and antigen-specific therapies (12-15). Unfortunately, these therapies have shown limited clinical benefit to date. To improve outcomes, therapies directed towards molecular targets specifically involved in T1D are needed.

In many autoimmune disorders, genes within the HLA complex confer disease risk (16). Alleles of the polymorphic class II genes, DQ and DR (and to a lesser extent DP), are the most important determinants of disease risk. These genes encode MHC proteins located on B-cells, dendritic cells, and macrophages that present processed antigens to CD4 T-cells. The MHC class II–peptide–T-cell receptor (TCR) forms a trimolecular complex involving the presentation of self-peptides shaping autoreactive T-cell responses in autoimmunity. Strong HLA disease associations exist for narcolepsy which only develops in individuals with HLA-DQ6 (DQB1*06:02) (17), Celiac disease is predominantly restricted to DQ2 and a lesser extent DQ8 (18), DR3 is present in 90% of neuromyelitis optica patients (19), multiple sclerosis is strongly associated with DR15 (20), and specific DR4 subtypes are present in rheumatoid arthritis (21, 22).

For T1D, the HLA-DQ8 allele (DQA1*03:01-DQB1*03:02) is present in 50-60% of all patients and provides an odds ratio for disease development of 6.5-11 (23-25). This is in stark

contrast to HLA-DQ6 (DQB1*06:02), which confers dominant protection with an odds ratio of 0.03 (25). The dichotomy of risk between the two alleles highlights the importance of MHC II antigen presentation within T1D development. Importantly, T-cells restricted to proinsulin peptides presented by DQ8 have recently been identified from the inflamed pancreatic islets of recent-onset T1D organ donors (26, 27), implicating DQ8 restricted T-cells in T1D pathogenesis. This evidence renders DQ8 an attractive therapeutic target to modify the autoimmune response, and we hypothesized that blocking DQ8 antigen presentation would represent a novel pathway for treating T1D.

Previously, we used molecular docking to screen a large chemical library of drug-like small molecules to predict those capable of occupying one of four structural pockets (P1, P4, P6 and P9) in the NOD mouse MHC II, I-A^{g7}, peptide-binding groove (28). The NOD mouse is a spontaneous model of autoimmune diabetes and shares similarities with human disease including MHC II genes conferring disease risk, development of insulin autoantibodies, and T-cell infiltration within pancreatic islets (29). Several compounds identified by in silico molecular docking were able to block insulin peptide binding to I-A^{g7} and subsequent T-cell activation in vitro (28).

In this study, we extended this approach for the purpose of inhibiting DQ8 antigen presentation. The crystal structure of DQ8 was used for molecular docking to select small molecules, which were then tested with in vitro bioassays and in preclinical animal models. By screening known drugs, we discovered methyldopa, a clinically well-established antihypertensive drug, specifically blocked DQ8 and subsequent T-cell responses. Methyldopa was used to treat recent-onset T1D patients with the DQ8 allele having residual beta cell function in an open-label clinical trial. Treatment resulted in the specific inhibition of DQ8 presentation by peripheral blood mononuclear cells (PBMCs) and a reduction in primary antigen-specific T-cell responses toward

insulin. The concept of blocking specific MHC II antigen presentation has significant relevance for T1D and other autoimmune diseases strongly associated with HLA alleles.

RESULTS

Molecular docking to select HLA-DQ8 binding small molecules

An in silico screening approach was used to rank small molecules predicted to bind structural pockets in the DQ8 peptide-binding groove. The sites within the antigen-binding cleft selected for molecular docking were based on the crystal structure of insulin B:11-23 bound to DQ8 (Supplemental Figure 1), which showed that the majority of intramolecular hydrogen bond interactions between peptide and HLA occurred between P1, P4, P6 and P9 side chains (30). We rationalized that drug binding to DQ8 in the sites critical for peptide binding would block antigen presentation and therefore used molecular docking to screen the P1, P4, P6 and P9 sites using a library consisting of 139,735 small molecules (Figure 1A). Each compound in the repository was docked in 1000 orientations within a single pocket, and scored based on the sum of attractive and repulsive intermolecular forces to estimate the predicted free energy of binding (ΔG). None of the top 40 scoring compounds overlapped between P1, P4, P6 and P9 (chemical structures, ΔG and in silico rank listed in Supplemental Tables 1-4 for each pocket), indicating distinct chemical composition and geometry among structural pockets in the DQ8 binding cleft.

Screening lead candidate small molecules with a bioassay

For each site, the top scoring compounds were tested for their ability to alter an insulin/DQ8-specific T-cell response in vitro. To establish a robust and reproducible T-cell bioassay, the TCR α/β genes of an insulin/DQ8 restricted T cell clone (named Clone 5) (31) was retrovirally expressed

on an immortalized T-cell devoid of endogenous TCR expression, thus creating a TCR transductant that secretes IL-2 when stimulated with insulin B:9-23 presented by DQ8. The use of an immortalized T-cell transductant allowed us to screen hundreds of small molecules and further evaluate 'hits' for specificity. Screening the top scoring compounds indicated that some molecules blocked T-cell responses, specifically 109 of 142 tested compounds, and two increased response above peptide alone; one increased response without peptide (Supplemental Table 4) and the other required peptide (Supplemental Table 1). The high frequency of active compounds predicted to bind P4 and P6 (34/34 for P4 and 33/34 for P6, Figure 1B) was in stark contrast to our previous efforts for murine I-A^{g7} in which only 5/160 tested compounds blocked an insulin specific T-cell response ($p<0.001$ comparing DQ8 versus I-A^{g7} inhibitory compounds using a Fisher's test). Evaluating chemical structures of compounds targeting P4 and P6 indicated a tetraaza core chemical structure existed for compounds selected by the P6 structural pocket, (tetraazatricylclododecane, TATD, Figure 2A) was present in 12/34 compounds (Supplemental Table 3). We synthesized this compound at high purity and measured the concentration required to block Clone 5 and another TCR transductant (489) restricted to a deamidated α-gliadin peptide presented by DQ8 (T-cell clone from a Celiac disease patient) (32). TATD inhibited both TCRs with nanomolar IC_{50} values and lower IC_{50} values for insulin compared to the post-translationally modified α-gliadin epitope (Figure 2B), which has a high binding affinity for DQ8 upon deamidation (Q→E). To exclude off target effects of TATD inhibiting a T-cell response, TATD was incubated with recombinant α-gliadin/DQ8 protein and free α-gliadin peptide in conditions to allow peptide exchange, washed, and then used to stimulate the 489 TCR (Figure 2C). These data demonstrated that TATD directly interacted with peptide/DQ8 complex. Furthermore, TATD did

not cause cell cytotoxicity (Supplemental Figure 2A) or inhibit a CD3 stimulated T-cell (Supplemental Figure 2B) at micromolar concentrations.

Preclinical studies in the NOD mouse

To evaluate whether blocking MHC II antigen presentation prevents autoimmune diabetes, TATD was administered to NOD mice. TATD cross-reacted with NOD I-A^{g7}, as an isomer was previously identified to block peptide binding and T-cell activation (28). In vivo administration early in the NOD disease course delays diabetes onset and prevents disease in half of the treated mice (Figure 2D). As CD4 T-cells undergo cognate interactions with B-cells, which can result in antibody production, we measured insulin autoantibodies in these mice. TATD treatment prevented insulin autoantibody production throughout the life of treated mice (Figure 2E). Treatment later in the NOD disease course resulted in maintenance of normal blood glucoses compared to PBS and similar to treatment with an anti-CD3 mAb, a positive control (Figure 2F and Supplemental Figure 3). Additionally, TATD treatment resulted in preserved glucose tolerance (Figure 2G) and less invasive islet immune cell infiltration compared to PBS treated mice (Figure 2, H and I).

Overall, these data indicate that therapeutic blocking of MHC II antigen presentation in a spontaneous model of autoimmune diabetes prevents disease onset, blocks critical interactions between T and B-cells, lessens tissue-specific destruction and maintains glucose tolerance when administered in later stages of diabetes development.

Screening FDA approved drugs to HLA-DQ8

Since in vitro and preclinical NOD studies suggested that small molecules binding pockets within the DQ8 antigen-binding cleft could be identified by molecular docking, we screened 1,207 FDA

approved small molecule drugs predicted to occupy the P6 pocket in an attempt to repurpose an existing drug. Of the top 39 scoring drugs (Supplemental Table 5), 10 out of 39 (25.6%) blocked Clone 5 (Supplemental Figure 4). One of these, methyldopa (Aldomet, Figure 3A) inhibited T-cell responsiveness in vitro. Methyldopa is a clinically well-established oral drug used in both children and adults to treat hypertension for more than 50 years (33), which provides an opportunity to repurpose methyldopa for immune-mediated treatment of T1D.

Methyldopa directly binds HLA-DQ8 and blocks antigen presentation in vitro

Methyldopa blocks in vitro DQ8 restricted T-cell responses to both Clone 5 (Figure 3B) and 489 (Figure 3C) in a dose dependent manner with IC_{50} values in the low micromolar range. There was no in vitro cell cytotoxicity and methyldopa was specific for inhibiting DQ8 restricted T-cell responses while not changing a DR4 restricted T-cell response (Figure 3D). DQ8 and DR4 are in close linkage disequilibrium on chromosome 6 and both class II molecules were present on APCs used for these studies. We next tested methyldopa to a panel of four TCRs restricted to the same deamidated α-gliadin peptide presented by DQ8 (34); only the TCR sequence was different between these transductants. Despite different levels of stimulation to peptide alone, methyldopa inhibited all four of the TCRs to varying degrees (Supplemental Figure 5). Methyldopa did not block a DQ8 restricted T-cell response to a viral peptide ($HA_{102-118}$) up to concentrations as high as 200 μM (Figure 3E). These data demonstrate that methyldopa inhibited antigen presentation by DQ8 in a peptide sequence-specific manner that may be related to peptide affinity for DQ8 and/or peptide sequence.

To ensure methyldopa directly interacts with DQ8 and assess drug-target biochemical interactions in vitro, we used isothermal titration calorimetry (ITC). ITC directly measures changes

in temperature that occur during fluid phase protein-ligand interaction (forming or breaking noncovalent interactions) and measures binding affinity as well as enthalpy and entropy. Figure 3F shows the heat released as methyldopa is titrated into DQ8 protein over time (upper panel) and the fitted binding curve (lower panel). With methyldopa being a small molecule (MW<500), there is very low but favorable enthalpy (negative ΔH), which derives from changes in interatomic interactions such as hydrogen bonding, van der Waals and electrostatic interactions. However, entropy of the reaction (removal of solvent molecules from the binding interface) is very favorable (positive ΔS) leading to a ΔG and K_D = 26.2 ± 4.2 μM similar to those reported for TCRs interacting with peptide/MHC (35).

Using the crystal structure of DQ8, we modeled methyldopa interacting with amino acid residues of the DQ8 alpha and beta chains within the antigen-binding cleft (Figure 3G). Two hydrogen bonds are predicted between methyldopa and DQ8 amino acid side chains. Testing structurally related compounds indicated that the modelled hydrogen bonds were indeed important to inhibit a TCR response, as removal of a hydroxyl group on the benzene ring or removal of the carboxylic acid abrogated the response (Table 1 and Supplemental Table 6). Further insights from the structure activity relationships indicate that a hydroxyl group on the benzene ring is a hydrogen bond donor to DQα62 asparagine and the carboxylic acid is a hydrogen bond acceptor for DQβ30 tyrosine.

Next, to determine whether methyldopa acts on the cell surface of APCs to displace peptides or intracellularly block peptide loading onto DQ8, we glutaraldehyde-fixed DQ8 APCs to inhibit intracellular antigen processing. Methyldopa inhibited T-cell activation with fixed APCs to a similar degree as with unfixed cells, indicating the main mechanism is through displacing cell surface peptides (Supplemental Figure 6, A and B). It is hypothesized that self-antigens are lower

affinity than foreign-antigens for MHC molecules and we therefore designed experiments to test whether methyldopa more effectively blocks lower affinity peptides. First, we tested the 489 TCR with wild-type α-gliadin peptide and the peptide with deamidation (Q→E) at P1 (p1E), P9 (p9E) or both (p1E/p9E). Deamidation facilitates anchoring of the peptide to DQ8, thereby increasing T-cell response to the gliadin/DQ8 complex. As expected, there was a hierarchy of responses, p1E/p9E > p9E > p1E > wild type (Supplemental Figure 6C). We then performed the same peptide titration experiment with methyldopa at a fixed concentration. Methyldopa blocked peptide presentation of lower affinity peptide/DQ8 complexes to a greater extent than higher affinity peptide/DQ8 complexes (Supplemental Figure 6D). These data are consistent with our observation that methyldopa was not able to block the T-cell response to a high affinity influenza peptide presented by DQ8 (Figure 3E).

Together, these data suggest a mechanism in which methyldopa binds directly within the DQ8 antigen-binding cleft on the cell surface to inhibit presentation of peptides to T-cells. Methyldopa was able to block peptides that bound DQ8 with lower affinities (i.e. insulin B:9-23) to a greater extent compared to peptides with higher DQ8 affinities.

Methyldopa blocks DQ8 antigen presentation in vivo

The in vivo effects of methyldopa were evaluated using DQ8 transgenic mice, as methyldopa does not block NOD I-A^{g7} restricted T-cell responses. Using these transgenic mice, we developed a biomarker assay to monitor the effect of methyldopa on DQ8 presentation (Figure 4A). Transgenic DQ8 mice were treated orally with vehicle or methyldopa at human equivalent doses, then their ex vivo splenocytes were used as APCs to stimulate Clone 5 and 489 with in vitro added peptide. The effects of methyldopa to block DQ8 antigen presentation in transgenic mice were dose

dependent (Supplemental Figure 7) and had to be administered multiple times each day as the plasma $t_{1/2}$ is 2 hours. When dosing multiple times a day, we observed a >50% reduction in T-cell responses with methyldopa (Figure 4B), while there were no changes in splenic $CD11b^+$ and $CD11c^+$ cell percentages or numbers (Figure 4 C and D). Additionally, there were no changes to cell surface DQ8 expression on these APCs (Figure 4E), indicating that methyldopa remains bound to DQ8 and inhibits TCR recognition of a peptide/DQ8 complex ex vivo.

Methyldopa is metabolized in the liver to α-methylnorepinephrine, which is responsible for blood pressure lowering by agonizing central α_2 adrenergic receptors (36). The metabolite did not inhibit DQ8 antigen presentation in vitro or in vivo (Supplemental Figure 8), demonstrating intact methyldopa is needed to interact with DQ8.

Methyldopa specifically blocks DQ8 antigen presentation in recent-onset T1D patients

We translated these preclinical findings to human T1D in a single-arm open-label phase 1b dose escalation study. We evaluated methyldopa treatment in 20 DQ8 positive T1D participants, ages 18-46 years with <2 years of diabetes duration who continued to produce endogenous insulin (Table 2 and Supplemental Table 7). All participants received methyldopa tablets orally at three separate dosages titrated over a 6-week period to prevent hypotension and assess different doses to block antigen presentation (Supplemental Figure 9). Methyldopa was well-tolerated and there were no serious adverse events.

The primary endpoint was the change from baseline DQ8 antigen presentation by PBMCs after 6-weeks of methyldopa treatment. Similar to the assay used to measure DQ8 antigen presentation in transgenic mice, primary PBMCs were used as APCs to present peptide to a cognate TCR transductant with secreted IL-2 measured after overnight culture (Figure 5, A-C). DQ8 T-

cell responses from 489 were inhibited while drug was administered and returned to baseline 6-weeks after stopping therapy (Figure 5D). There is statistically significant inhibition with low, moderate and high doses of methyldopa. Clone 5 responses were also blocked out to 1-week after stopping therapy (Figure 5E). DQ8 presentation was inhibited 40% compared to baseline levels with 17/20 patients responding (Supplemental Figure 10 for individual responses); one non-responder did not have detectable plasma methyldopa levels (Supplemental Figure 11) and two were DQ8 homozygotes. There appears to be a DQ8 dose effect as higher drug doses were required to block response in homozygotes (n=4) compared to heterozygotes (Supplemental Figure 12).

As a control, DR4 antigen presentation was measured as it is present on APCs with DQ8. DR4 presentation was not significantly affected in study participants (p=NS, Figure 5F). In addition, DQ2 (DQB1*02:01) antigen presentation was not altered in participants with this MHC II molecule (Figure 5G). Flow cytometric analysis of PBMCs indicated similar numbers of APCs (B-cells, myeloid DCs, plasmacytoid DCs) with no change in the mean fluorescence intensity of DQ or DR on the cell surface throughout the study (Supplemental Figure 13).

Together, these results indicate methyldopa treatment specifically inhibits DQ8 antigen presentation while drug is administered and function returns to normal upon withdrawal of therapy.

Methyldopa reduces insulin-specific CD4 T-cell response in the peripheral circulation

To measure primary T-cell responses, as opposed to antigen presentation described above, indirect IFN-γ enzyme linked immunospot (ELISPOT) assays were performed on cryopreserved samples using an insulin B:9-23 (B22E) mimotope which is presented by DQ8 (37, 38). Seven study subjects responded at baseline and responses decreased at study completion (Figure 6A). This was not the case for whole tetanus toxin (Figure 6B) or DR4 epitopes within the protein (Figure 6 C

and D) (39). Additionally, we have shown that the tested insulin epitope activates human CD4 T-cells isolated from the inflamed islets of T1D organ donors (26), highlighting the importance of blocking this reactivity in T1D patients.

Methyldopa treatment results in good glycemic control and maintains beta cell function over 3-months

Participants had good glycemic control at study conclusion with hemoglobin A1c levels averaging 6.5% (Figure 7A), with no change in total insulin doses (Figure 7B). A measure of residual endogenous insulin production, C-peptide 2 hour AUC following a mixed meal tolerance test, at 3-months was similar to baseline levels (Figure 7C). From natural history studies it is appreciated that there is a steady decline in C-peptide AUC after diagnosis, and age-matched historical controls would be expected to have ~30% loss one year after diagnosis (40). Although short-term, these results suggest methyldopa treatment may limit beta cell destruction and preserve function; however, trials with a longer duration and placebo arm are needed to fully evaluate metabolic efficacy.

DISCUSSION

Preventing pathogenic T-cell receptor activation by self-antigen/MHC class II complexes may provide a novel means to prevent and potentially reverse T1D and other autoimmune conditions. In this report, we used a rational structure-based approach to evaluate the 'druggability' of pockets in the antigen-binding cleft of the T1D risk HLA-DQ8 molecule. Our goal was to identify drug candidates that occupy specific structural pockets and inhibit antigen presentation to T-cells. Using the crystal structure of DQ8 as the basis for selection of candidate small molecules

from a large chemical library, we show that DQ8 is remarkably amenable to drugs targeting pockets along the antigen-binding cleft, especially the P4 and P6 pockets. We then screened FDA approved drugs predicted to bind the P6 pocket in an attempt to repurpose an existing drug. We tested drugs in vitro, in vivo, and in humans to show that methyldopa specifically and durably blocked DQ8 antigen presentation. Moreover, methyldopa reduced inflammatory insulin-specific T-cell responses when administered to recent-onset T1D patients in a proof of concept trial. Longer-term placebo controlled trials are warranted to evaluate methyldopa in potentially preserving residual β-cell function in those at-risk and with new-onset T1D.

In our clinical trial treating recent-onset T1D patients with methyldopa, we observed a 40% reduction in DQ8 antigen presentation when using PBMCs as APCs (Figure 5D). Presumably methyldopa is sequestered within DQ8 on DCs, B-cells and monocytes that are capable of presenting in vitro added peptide to our engineered TCR transductants. Our data indicates that this is plausible as methyldopa directly binds isolated DQ8 protein (Figure 3F) and interacts with cell surface DQ8 as opposed to intracellular peptide loading. In fact the processes of PBMC isolation, freezing, thawing and washing cells does reduce the amount of inhibition measured with this assay (Figure 5A), likely resulting in a loss of DQ8 sequestered methyldopa, indicating that a 40% reduction may be an under representation of what occurs directly in vivo. Despite this limitation, DQ8 is blocked while methyldopa therapy is administered and returns to baseline levels upon withdrawal of therapy. This pattern of drug treatment effect is not present for DR4, which is present on APCs with DQ8. Additionally, DQ2 presentation is not blocked with methyldopa treatment. This data demonstrates the specificity of methyldopa between MHC II molecules and within DQ types. It is important to note that other MHC class II molecules, i.e. DR4, DR3, DQ2 and DQ8-trans (composed of the DQ2 alpha and DQ8 beta chain), can present diabetes relevant peptides

(41). As there is epitope spreading that occurs during T1D pathogenesis, timing of therapeutic intervention with methyldopa to block DQ8 in the disease course is an important consideration where those at earlier stages of disease could potentially have more clinical benefit.

Another observation from our data is that the methyldopa IC_{50} values to inhibit T-cell responses to insulin and gliadin are in the low micromolar range (3-50 μM). Using a separate technique to assess biochemical interactions (ITC) provided very similar results with an average K_D of 26 μM. Of particular interest is the fact that these values are in the reported range of affinities for TCRs binding to peptide/MHC as measured by surface plasmon resonance and ITC (35, 42, 43). Despite these somewhat low affinity interactions of methyldopa with DQ8, primary autoantigen specific T-cell responses decreased in a subset of patients responding to an insulin B chain mimotope (Figure 6A). Fife and colleagues recently determined the phenotype of these T-cells directly ex vivo from peripheral blood in recent-onset T1D patients using fluorescent tetramers. These insulin specific T-cells were antigen experienced and predominantly an effector memory or central memory phenotype (44). Future studies will be directed to determine whether these insulin specific T-cells become anergic or are deleted with methyldopa treatment.

In addition to small molecule drugs that occupy structural pockets in disease-related HLA molecules, there are alternate therapies to inhibit HLA-specific antigen presentation including antibodies targeting specific HLA molecules or peptide/HLA complexes. Although serotype-specific anti-HLA antibodies are available, their lack of specificity towards single HLA molecules would likely result in more off-target effects compared to an allele specific agent. Moreover, it is difficult to generate allele-specific antibodies, as key polymorphisms that distinguish closely related molecules encode amino acid differences at sites within the antigen-binding cleft that are inaccessible to antibodies. Monoclonal antibodies for specific peptide/MHC molecules have been

generated (45, 46), but are only specific for single epitopes, while immune responses to many different self-antigens are present in an autoimmune disease. Small molecule drugs have not been widely utilized to target HLA molecules, as ligands for conventional polymorphic HLA molecules have primarily been described as peptides. Until recently, small molecules were not thought to bind in the antigen-binding cleft. The anti-retroviral drug abacavir was shown to directly interact with a structural pocket (F pocket, P9 or PΩ) in the peptide binding cleft of HLA-B*57:01 by X-ray crystallography (47, 48). This data, along with our results presented here, suggest that specific pockets within MHC class I and II antigen-binding grooves have chemical and geometric features amenable to binding small molecules.

Several concerns exist with using small molecule drugs to target MHC II antigen presentation. First, negative effects on immune function may result from a hole in the immune repertoire created when a specific MHC II molecule is blocked. However, detrimental effects on immune function are not expected, as other class II molecules exist to provide normal adaptive immune responses. For methyldopa, DQ8 restricted T-cell responses to lower affinity self-antigens were inhibited while those to a higher affinity viral pathogen remained unaltered. Additionally, DR4 and DQ2 responses remain intact; it is also likely that DP functions normally.

Second, drugs may trigger unwanted immune responses (hypersensitivity) by binding specific HLA molecules and creating neoantigen epitopes. Adverse drug reactions can be severe, but are rare (1-2/1,000,000 for Stevens-Johnson Syndrome and 0.4-1.2/1,000,000 each year for Toxic Epidermal Necrolysis) and have been identified only after treating large numbers of patients with the offending drug (49). Moreover, the modest affinity of methyldopa for DQ8 (K_D ~26 μM) is significantly lower than a drug that caused hypersensitivity in a HLA associated manner, abacavir bound a self-peptide and HLA-B*57:01 with an estimated K_D of 0.2 nM (50). These data

suggest that methyldopa is not likely to bind DQ8 with sufficient affinity to alter the repertoire of peptides and consequent presentation of neoantigens that trigger hypersensitivity.

One advantage of "repurposing" existing drugs is that well-characterized safety profiles indicate potential complications and off-target effects. The safety profile of methyldopa, which is on the World Health Organization's list of Essential Medicines, is based on over 50 years of clinical use and is indicated for treatment of pregnancy-induced hypertension. Since HLA-DQ8 is present in European Americans at a frequency of ~10% (51), methyldopa has been administered to large numbers of individuals expressing DQ8 and is considered safe.

In conclusion, we describe a novel approach to identify immunomodulatory small molecules targeted to DQ8. As many autoimmune diseases are associated with specific HLA alleles and high resolution crystal structures exist for many of these MHC class II molecules, rapid strategies to select HLA allele-specific compounds and test activities in experimental systems can occur. The ability to identify HLA allele-specific drugs has broad applicability to treating autoimmunity and other HLA-associated conditions.

METHODS

Molecular modeling and docking

We used the crystal structure of HLA-DQ8 complexed to insulin B:11-23, Protein Data Bank code 1JK8, as the basis for molecular docking (52). To prepare the site for docking, all water molecules were removed and protonation of DQ8 residues was done with SYBYL (Tripos) (53). The molecular surface of the structure was explored using sets of spheres to describe potential binding pockets. The sites selected for molecular docking were defined using the SPHGEN program (generates a grid of points that reflect the shape of the selected site) and filtered through

CLUSTER. The CLUSTER program groups the selected spheres to define the points that are used by DOCK v5.1.0 (54) to match potential ligand atoms with spheres. Intermolecular AMBER energy scoring (van der Waals + columbic), contact scoring, and bump filtering were implemented in the DOCK program algorithm. Atomic coordinates for 139,735 small molecules in the NIH Developmental Therapeutics Program repository of drug-like compounds were positioned in each structural pocket in 1000 different orientations and scored based on predicted polar (hydrogen bond) and nonpolar (van der Waals) interactions. The most favorable orientation and scores (contact and electrostatic) were calculated. PYMOL was used to generate graphic images.

Generation of T-cell receptor transductants

TCR transductants were generated as previously described using retroviral transduction of the 5KC murine T-cell hybridoma cell line lacking endogenous TCR expression (55). The sequences for the α/β TCR clones either came as kind gifts from investigators [Clone 5 from Bart Roep (Leiden University, Leiden, Netherlands), 489 from Ludvig Sollid (Oslo University, Oslo, Norway), DQ8-flu from Bill Kwok (Benaroya Research Institute, Seattle, Washington, USA)] or published literature (clones 13, 22 and 38 which are DQ8 restricted; clone 233 which is DQ2 restricted; C7CH17 which is DR4 restricted) (31, 32, 34, 56). Supplemental Table 9 lists each TCR transductant, corresponding peptide and MHC class II restriction. Briefly, to create a TCR transductant, a single TCR sequence (α and β chains linked by the PTV1.2A sequence) was cloned into MSCV-based retroviral vectors carrying green fluorescent protein (GFP) (pMIGII) or pMSCV puro retroviral vector (Clontech), followed by production of replication-incompetent retroviruses encoding TCR sequences. 5KC cells transduced with retroviruses were then selected either by flow cytometric cell sorting of GFP positive cells or with puromycin according to the selection genes carried by the retroviral vectors; TCR expression was confirmed by staining with anti-mouse

TCRβ antibody (BD Biosciences, clone H57-597). The 5KC cells were also transduced to express native human CD4, which was confirmed by flow cytometric staining with an antibody against CD4 (BioLegend, clone RPA-T4).

In vitro screening of small molecules

Small molecules for screening were obtained from the NIH/DTP repository in vialed sets, dissolved in DMSO and diluted in PBS for a final concentration of 0.1% DMSO in each well. Each small molecule was screened at a concentration of 100 μM. The clone 5 TCR transductant was cultured with peptide +/- small molecule in the presence of murine DQ8-transgenic spleen cells. DQ8-transgenic spleen cells were dispersed to single cells, followed by red blood cell lysis and then $2x10^5$ splenoctyes were cultured with peptide for 4 hours in a 96-well U-bottom plate followed by the addition of $2x10^5$ Clone 5 cells for overnight culture. Murine IL-2 secreted by the 5KC cells was measured using a highly-sensitive ELISA (V-PLEX IL-2 kit, Meso Scale Diagnostics, LLC) followed by detection on the MESO QuickPlex SQ120 instrument. Pocket 1 and 9 small molecules were screened using Clone 5 in the presence of insulin B:9-23 (100 μg/ml), while pocket 4 and 6 compounds used insulin B:13-23 (100 μg/ml) which provides a higher amount of IL-2 secretion than B:9-23.

Peptides, protein and small molecules

Peptides used for TCR stimulation assays were obtained from Genemed Synthesis Inc. at > 95% purity. Recombinant α-gliadin/DQ8 protein containing the following deamidated peptide sequence (QQYPSGEGSFQPSQENPQ) was expressed in S2 drosophila cells and purified as previously described (55). TATD (1,3,6,8-Tetraaza-tricyclo[4.4.1.13,8]dodecane) was synthesized at > 95% purity and characterized by ^{1}H NMR and ^{13}C NMR (The Chemistry Research Solutions, LLC). Methyldopa was purchased at > 98% purity (Sigma Aldrich, catalog 857416), the metabolite α-

methylnorepinephrine (Toronto Research Chemicals Inc., catalog D454000) and structurally related compounds to methyldopa from Sigma Aldrich. DQ8 protein used for ITC was isolated and purified by affinity chromatography using a DQ mAb (clone SPV-L3) and an EBV transformed B-cell line derived from a DQ8 homozygote (57).

Characterization of TATD in vitro

TATD was dissolved in PBS and stored in low binding eppendorf tubes (Costar, catalog 3207). Dose titrations were performed in a similar manner to the small molecule screening assays: $2x10^5$ DQ8-transgenic splenocytes were culture with cognate peptide (100 μg/ml B:13-23 for Clone 5 and 1 μM deamidated α-gliadin for TATD) for 4 hours, followed by the addition of $2x10^5$ TCR transductant cells for overnight culture and measurement of secreted IL-2. Cell viability was measured with the CellTiter-Glo Luminescent assay (Promega) following manufacturer instructions. Experiments with recombinant deamidated α-gliadin/DQ8 protein were performed by incubating 0.01 μg protein in 100 μl of buffer (25 mM sodium phosphate at pH=8.0) with 1 μM deamidated α-gliadin peptide plus TATD concentrations for 24 hours at 50°C to allow peptide exchange. Following the initial incubation, contents were transferred to a 96-well high binding plate (Costar, catalog 9018) and incubated for 2 hours at room temperature. The plate was washed twice with 0.05% Tween-20 in PBS to remove any unbound protein, peptide and TATD. Then, 10^5 489 cells were incubated with the protein overnight at 37° with 5% CO_2, the supernatant was assayed for secreted IL-2.

Characterization of methyldopa in vitro

Methyldopa was dissolved in dilute HCl and pH adjusted to 7.0 prior to each in vitro assay being performed, as air oxidation was visible over the ensuing days. Dose titrations with TCR transductants were performed in an identical manner to those done with TATD. To assess in vitro

specificity, EBV transformed B-cells from a DQ8/DR4 homozygote (DQA1*03:01-DQB1*03:02-DRB1*04:01) were used as APCs (57). For these assays, 10^5 EBV transformed B-cells were cultured with cognate peptide for 4 hours, followed by the addition of 10^5 TCR transductant cells for overnight culture and measurement of secreted IL-2. For experiments done with the DQ8-flu TCR, previously produced M12C3 cells (murine B-cell line) expressing HLA-DQ8 were used as APCs ($5x10^4$) (26), cultured with 10 μg/ml of influenza peptide for 4 hours, followed by the addition of TCR transductant (10^5) for overnight culture and measurement of secreted IL-2. To assess the effects of intracellular uptake of methyldopa, APC fixation experiments were conducted. M12C3 DQ8 cells were glutaraldehyde fixed. To fix cells, these APCs ($5x10^6$/ml) were incubated with 0.05% glutaraldehyde for 30 seconds, followed by quenching the reaction with 0.2 M glycine. Fixed APCs ($5x10^4$) were cultured with 10 μM of deamidated α-gliadin peptide and methyldopa for 24 hours and then 489 TCR transductant (10^5 cells) added for overnight culture followed by the measurement of secreted IL-2.

Isothermal Titration Calorimetry

ITC experiments were performed using a Microcal ITC200 calorimeter (GE Healthcare) at 25°C. DQ8 protein was dialyzed in citrate-phosphate buffer (pH=5.0) and loaded into the calorimeter cell at a concentration of 4 μM. Methyldopa was dissolved in the same citrate-phosphate buffer at a concentration of 4 mM and pH adjusted to 5.0. Injection volumes of methyldopa were 2 μl every 4 minutes over a total of 80 minutes. The first data point was removed from analysis due to dilution across the injection needle tip. Binding isotherms were generated using Origin Software (Microcal, Inc.) with a single-site binding model by nonlinear regression. For baseline correction, methyldopa was titrated into buffer prior to each experiment and subtracted from each data set. Dissociation

constants (K_D) were calculated as the reciprocal of the measured binding affinity and free energy of binding was calculated from the equation $\Delta G = \Delta H - T\Delta S$.

Animals

Mice were bred and housed under specific pathogen-free conditions at the University of Colorado Denver Center for Comparative Medicine. Female NOD mice were purchased from Jackson Laboratories and used for the early and late intervention studies with TATD. The late prevention study, therapy beginning at 12 weeks of age, was conducted at Novartis Research Facilities in Basel, Switzerland. TATD was dissolved in PBS for intraperitoneal administration and sterile water for oral gavage. An anti-CD3 mAb (eBioscience, clone 2C11) was administered by intraperitoneal injection at 50ug daily for five consecutive days in the late prevention study.

DQ8 transgenic mice (containing a human DQ8/CD4 transgene, murine IA-null on a NOD Rag KO background) were obtained from Jackson Laboratories (catalog 006022) and bred at the University of Colorado Denver. Spleens from these mice were used for splenocytes to present peptides to TCR transductants in in vitro T-cell stimulation assays and for in vivo testing of methyldopa and metabolites. DQ8 transgenic mice were used on a Rag KO background such that T and B-cells would not be present to secrete IL-2. For the in vivo studies with methyldopa, methyldopa powder was dissolved in dilute HCl prior to each administration and control mice received dilute HCl (vehicle).

Assessment of murine diabetes, insulin antibodies, and glucose tolerance testing

Blood glucose was measured weekly with a Reli On blood glucose monitoring system (Solartek), and mice were considered diabetic after two consecutive blood glucose values >250 mg/dl (13.9 mmol/L). Insulin antibodies were measured with a fluid phase radioimmunoassay at 4 weeks of age and then every 4 weeks thereafter as previously described (58). Intraperitoneal glucose

tolerance tests were performed following an overnight fast, D-glucose (2 g/kg body weight) was administered by intraperitoneal injection in 200 µl PBS. Blood glucose values were obtained at 0, 15, 30, 60, 90 and 120 min using a Reli On meter, and 2 hour glucose AUC calculated.

Histological analysis

Parafin embedded pancreatic sections were H&E stained followed by insulin staining. Islets were identified by glucagon staining and graded for insulitis by an individual blinded to the experimental design. At least 100 islets per cohort (PBS or TATD) were scored for islet infiltration as follows: 0, no infiltration; 1, peri-insulitis; 2, islets with lymphocyte infiltration in less than 50% of the area; 3, islets with lymphocyte infiltration in more than 50%.

Study patients and assessments

For the phase 1b dose escalation study, subjects were recruited from the Barbara Davis Center for Diabetes clinics. Eligibility criteria included: 1) ages 18-45 years, 2) diagnosed with T1D by American Diabetes Association criteria for less than 2 years, 3) positive for at least one T1D-related autoantibody (insulin autoantibodies only considered positive if measured within three weeks of starting exogenous insulin therapy), 4) positive for at least one DQ8 allele (DQB*03:02), and 5) a random serum C-peptide level greater than 0.1 nmol/L, which is a measure of residual beta-cell function.

Visits and clinical assessments were performed at baseline and weeks 1, 3, 6, 7 and 12 for a total of six visits. Blood samples were obtained at each visit for immunologic assessments. PBMCs were isolated from heparinized blood using Ficoll-paque; freshly isolated PBMCs were used for flow cytometry panels to analyze peripheral blood B-cells and DCs, while the remainder were cryopreserved in FBS with 10% DMSO. Physical examination and metabolic samples (glycated hemoglobin [HbA_{1c}] and mixed meal tolerance tests [MMTT]) were obtained at baseline

and week 12. Pill counts were performed at visits on weeks 1, 3 and 6 to assess drug compliance. Adverse events and insulin use (basal and bolus) were recorded at each study visit.

Measuring serum islet autoantibodies and HLA genotyping

Peripheral blood was obtained for islet autoantibody assays and HLA genotyping. Islet autoantibodies to insulin, GAD65, IA-2, and ZnT8 were measured from the serum by fluid-phase RIA as previously described (59). HLA-DRB1, DQA1, and DQB1 alleles were typed using oligonucleotide probes as previously described (60).

Tolerability and safety of methyldopa

Methyldopa (Aldomet) 500 mg tablets were obtained from Mylan Pharmaceuticals (lot # 3038543 and 3062517). Study subjects self-administered doses throughout the open-label study. All participants tolerated the low dose (500 mg twice daily) and moderate dose (500 mg three times daily), while 18 out of 20 tolerated the high dose (2-3 grams divided daily). For the two individuals that did not tolerate the high dose, the moderate dose was continued during the treatment phase of the study. Methyldopa has a well-known safety profile and in our trial we observed: (1) no lowering of systolic or diastolic blood pressure, (2) no elevation of liver function tests (AST or ALT), and (3) no anemia. There were no serious adverse events related to study drug administration.

Immunologic assessments

Measuring specific MHC class II presentation – Cryopreserved PBMCs were thawed and $2x10^5$ cells cultured with peptide (200 μg/ml of B:13-23 for Clone 5, 10 μM deamidated α-gliadin for 489, 100 μM α-II-gliadin for 233, or 1 μg/ml $HA_{306-318}$ for C7CH17) in 96-well U-bottom plates for 4 hours at 37° with 5% CO_2. After 4 hours, the corresponding TCR transductant (10^5 cells) was added and incubated overnight at 37° with 5% CO_2. Each condition was done in triplicate wells

including no antigen and anti-CD3 (eBioscience, clone 2C11), which was a positive control for the TCR transductant. PBMCs from each study visit for a single participant were included on the same 96-well plate for each TCR transductant (i.e. PBMCs from each of the six visits were on a single plate for Clone 5) to avoid batch effects between study visits and participants. Following overnight culture, the plate was centrifuged at 500g for 5 min, supernatant removed and frozen at -80° until IL-2 in the supernatant was measured using a highly-sensitive ELISA (Meso Scale Diagnostics, LLC).

ELISPOT assays – assays were conducted as previously described using the human IFN-γ ELISPOT kits (UCyTech Biosciences) (61). Briefly, cryopreserved PBMCs were thawed and 10^6 cells cultured in 250 μl of serum free AIM-V® Medium (Invitrogen) with 10 μg/ml of peptide. Cells were supplemented with an additional 250 μl of medium after 24 hours, and harvested 24 hours later. After washing, the cells were resuspended in 300 μl medium and transferred as three 100 μl aliquots to 96-well clear polystyrene culture plates coated with an IFN-γ capture monoclonal antibody and subsequently treated with 1 x blocking solution (UCyTech). Seventeen hours later, the cells were removed by decanting, and the wells washed. Spots were then formed by sequential incubations with the biotinylated 2^{nd} site anti-IFN-γ, gold-labeled goat anti-biotin, and a precipitating silver substrate. Spots were enumerated with a Bioreader 4000 Pro X (BIOSYS GmbH). Wells with no antigen were a negative control and tetanus toxoid vaccine was used as a positive control in each assay.

Flow Cytometry - freshly isolated PBMCs were stained with cell surface markers for the following panels: B-cells (CD19, HLA-DR, HLA-DQ, myeloid DCs 1 (CD11c, CD1c [BDCA-1], HLA-DR, HLA-DQ, CD4/CD8), myeloid DCs 2 (CD11c, CD141 [BDCA-3], HLA-DQ, HLA-DQ, CD4/CD8) and plasmacytoid DCs (CD11c, CD303 [BDCA-2], CD304 [BDCA-4], CD123, HLA-

DR, HLA-DQ). Specific antibody clones and suppliers are listed in Supplemental Table 10; isotype controls were used for CD11c and CD123. Analysis was done using a Becton-Dickenson LSR-II and data analyzed using FlowJo Software (version 9).

Metabolic assessments

At time 0 and 3 months, HbA_{1c} was measured using a DCA2000 Analyzer (Siemens Healthcare Diagnostics). A MMTT (360 ml of Boost) was administered with serum C-peptide measured at time 0, 15, 30, 60, 90 and 120 min using an ELISA assay (ALPCO), and 2 hour C-peptide AUC calculated.

Plasma Methyldopa Levels

Methyldopa concentration was measured in 100 µl of cryopreserved sample (1:1 plasma:PBS) collected at each study visit. Samples were thawed, underwent protein precipitation with 25 µl of 10% perchloric acid in milli-Q water followed by centrifugation at 13,300g for 15 min, and supernatant was analyzed by liquid chromatography tandem mass spectrometry. Positive ion electrospray ionization mass spectra were obtained with a MDS Sciex 3200 Q-TRAP triple quadrupole mass spectrometer (Applied Biosystems, Inc.) with a turbo ion spray source interfaced to an Agilent 1200 Series Binary Pump SL HPLC system. Samples were chromatographed using a Sunfire C8, 5 µm, 4.6 x 50 mm column (Waters Corporation) protected by a C18 guard cartridge, 4.0 x 2.0 mm (Phenomenex). Methyldopa standard curves were prepared in human plasma diluted 1:1 spiked with 5 µl of appropriate standard concentration with PBS and were linear over the range of 5 to 5,000 ng/ml. The linearity of the standard curves was greater than $r^2 = 0.99$ using $1/x^2$ weighting.

Statistical analysis

Statistical analyses were performed using and SAS 9.4 (SAS Institute) and GraphPad Prism 6.0 software (GraphPad Software) including calculations for IC_{50} values from dose titrations with TATD and methyldopa. The statistical tests used for each experiment are indicated in the corresponding figure legend. P-values <0.05 are considered significant. For MHC class II specific antigen presentation in study subjects, longitudinal mixed-effects models adjusted for the baseline value were used to examine changes over time. Residual plots were examined in order to evaluate the fit of the models. P-values compare differences of least-squares means between two time points. For safety outcomes (blood pressure, liver function tests and hemoglobin), mixed-effects models were used to compare mean values on and off treatment, without adjustment for baseline.

Study Approval

Animal studies were conducted under approved protocols by the University of Colorado Denver and Novartis Animal Care and Use Committees. The clinical investigation in this study was conducted in accordance with the Declaration of Helsinki principles with study approval provided by the Colorado Multiple Institutional Review Board. The clinical trial (NCT01883804) was investigational new drug (IND) exempt by the FDA (PIND 118119). Written informed consent was obtained after the nature and possible consequences of the study were explained to each participant.

AUTHOR CONTRIBUTIONS

D.A.O, M.A.A., P.A.G. and A.W.M. designed the studies and wrote the manuscript. A.A., K.A.M., S.C. E.E.B., B.P. and K.J.S. performed experiments and reviewed the manuscript. L.P. conducted independent statistics on the study data. S.E., V.N.S, S.K.G., P.A.G. and A.W.M. designed, obtained regulatory approval and conducted the phase 1b clinical trial. A.W.M. is the guarantor of

this work, had full access to all the data in the study, and takes responsibility for the data integrity and accuracy of analysis.

ACKNOWLEDGMENTS

We thank the late George S. Eisenbarth (1942-2012) for helpful scientific discussions, inspiration, and encouragement. We also thank the National Cancer Institute (NCI)/Division of Cancer Treatment and Diagnosis (DCTD)/Developmental Therapeutics Program (DTP) for providing the small molecules used for screening in the study along with Lori Sussel and Edwin Liu at the University of Colorado for critical editing of the manuscript. This work was supported by NIH Grants (DK095995, DK108868, DK110845, DK032083, DK104223, AI110503); the Juvenile Diabetes Research Foundation (17-2010-744, 2014-143-C-R); the Children's Diabetes Foundation; the Barbara Davis Center Translational Research Unit; and the Colorado Clinical and Translational Science Institute (TR001082).

REFERENCES

1. Atkinson MA, Eisenbarth GS, and Michels AW. Type 1 diabetes. *Lancet.* 2014;383(9911):69-82.

2. Bluestone JA, Herold K, and Eisenbarth G. Genetics, pathogenesis and clinical interventions in type 1 diabetes. *Nature.* 2010;464(7293):1293-300.

3. Ziegler AG, Rewers M, Simell O, Simell T, Lempainen J, Steck A, et al. Seroconversion to multiple islet autoantibodies and risk of progression to diabetes in children. *JAMA.* 2013;309(23):2473-9.

4. Mayer-Davis EJ, Lawrence JM, Dabelea D, Divers J, Isom S, Dolan L, et al. Incidence Trends of Type 1 and Type 2 Diabetes among Youths, 2002-2012. *N Engl J Med.* 2017;376(15):1419-29.

5. Rigby MR, Harris KM, Pinckney A, DiMeglio LA, Rendell MS, Felner EI, et al. Alefacept provides sustained clinical and immunological effects in new-onset type 1 diabetes patients. *J Clin Invest.* 2015;125(8):3285-96.

6. Sherry N, Hagopian W, Ludvigsson J, Jain SM, Wahlen J, Ferry RJ, Jr., et al. Teplizumab for treatment of type 1 diabetes (Protege study): 1-year results from a randomised, placebo-controlled trial. *Lancet.* 2011;378(9790):487-97.

7. Keymeulen B, Vandemeulebroucke E, Ziegler AG, Mathieu C, Kaufman L, Hale G, et al. Insulin needs after CD3-antibody therapy in new-onset type 1 diabetes. *N Engl J Med.* 2005;352(25):2598-608.

8. Herold KC, Hagopian W, Auger JA, Poumian-Ruiz E, Taylor L, Donaldson D, et al. Anti-CD3 monoclonal antibody in new-onset type 1 diabetes mellitus. *N Engl J Med.* 2002;346(22):1692-8.

9. Pescovitz MD, Greenbaum CJ, Krause-Steinrauf H, Becker DJ, Gitelman SE, Goland R, et al. Rituximab, B-lymphocyte depletion, and preservation of beta-cell function. *N Engl J Med.* 2009;361(22):2143-52.

10. Orban T, Bundy B, Becker DJ, DiMeglio LA, Gitelman SE, Goland R, et al. Co-stimulation modulation with abatacept in patients with recent-onset type 1 diabetes: a randomised, double-blind, placebo-controlled trial. *Lancet.* 2011;378(9789):412-9.

11. Moran A, Bundy B, Becker DJ, DiMeglio LA, Gitelman SE, Goland R, et al. Interleukin-1 antagonism in type 1 diabetes of recent onset: two multicentre, randomised, double-blind, placebo-controlled trials. *Lancet.* 2013;381(9881):1905-15.

12. Wherrett DK, Bundy B, Becker DJ, DiMeglio LA, Gitelman SE, Goland R, et al. Antigen-based therapy with glutamic acid decarboxylase (GAD) vaccine in patients with recent-onset type 1 diabetes: a randomised double-blind trial. *Lancet.* 2011;378(9788):319-27.

13. Nanto-Salonen K, Kupila A, Simell S, Siljander H, Salonsaari T, Hekkala A, et al. Nasal insulin to prevent type 1 diabetes in children with HLA genotypes and autoantibodies conferring increased risk of disease: a double-blind, randomised controlled trial. *Lancet.* 2008;372(9651):1746-55.

14. Skyler JS, Krischer JP, Wolfsdorf J, Cowie C, Palmer JP, Greenbaum C, et al. Effects of oral insulin in relatives of patients with type 1 diabetes: The Diabetes Prevention Trial--Type 1. *Diabetes Care.* 2005;28(5):1068-76.

15. Diabetes Prevention Trial – Type 1 Diabetes Study Group. Effects of insulin in relatives of patients with type 1 diabetes mellitus. *N Engl J Med.* 2002;346(22):1685-91.

16. Tsai S, and Santamaria P. MHC Class II Polymorphisms, Autoreactive T-Cells, and Autoimmunity. *Front Immunol.* 2013;4:(321):1-7.

17. Inoko H, Ando A, Tsuji K, Matsuki K, Juji T, and Honda Y. HLA-DQ beta chain DNA restriction fragments can differentiate between healthy and narcoleptic individuals with HLA-DR2. *Immunogenetics.* 1986;23(2):126-8.

18. Green PH, and Cellier C. Celiac disease. *N Engl J Med.* 2007;357(17):1731-43.

19. Bukhari W, Barnett MH, Prain K, and Broadley SA. Molecular pathogenesis of neuromyelitis optica. *Int J Mol Sci.* 2012;13(10):12970-93.

20. Moutsianas L, Jostins L, Beecham AH, Dilthey AT, Xifara DK, Ban M, et al. Class II HLA interactions modulate genetic risk for multiple sclerosis. *Nat Genet.* 2015;47(10):1107-13.

21. Viatte S, Plant D, and Raychaudhuri S. Genetics and epigenetics of rheumatoid arthritis. *Nat Rev Rheumatol.* 2013;9(3):141-53.

22. Raychaudhuri S, Sandor C, Stahl EA, Freudenberg J, Lee HS, Jia X, et al. Five amino acids in three HLA proteins explain most of the association between MHC and seropositive rheumatoid arthritis. *Nat Genet.* 2012;44(3):291-6.

23. Hu X, Deutsch AJ, Lenz TL, Onengut-Gumuscu S, Han B, Chen WM, et al. Additive and interaction effects at three amino acid positions in HLA-DQ and HLA-DR molecules drive type 1 diabetes risk. *Nat Genet.* 2015;47(8):898-905.

24. Concannon P, Rich SS, and Nepom GT. Genetics of type 1A diabetes. *N Engl J Med.* 2009;360(16):1646-54.

25. Erlich H, Valdes AM, Noble J, Carlson JA, Varney M, Concannon P, et al. HLA DR-DQ haplotypes and genotypes and type 1 diabetes risk: analysis of the type 1 diabetes genetics consortium families. *Diabetes.* 2008;57(4):1084-92.

26. Michels AW, Landry LG, McDaniel KA, Yu L, Campbell-Thompson M, Kwok WW, et al. Islet-Derived CD4 T Cells Targeting Proinsulin in Human Autoimmune Diabetes. *Diabetes.* 2017;66(3):722-34.

27. Pathiraja V, Kuehlich JP, Campbell PD, Krishnamurthy B, Loudovaris T, Coates PT, et al. Proinsulin-specific, HLA-DQ8, and HLA-DQ8-transdimer-restricted CD4+ T cells infiltrate islets in type 1 diabetes. *Diabetes.* 2015;64(1):172-82.

28. Michels AW, Ostrov DA, Zhang L, Nakayama M, Fuse M, McDaniel K, et al. Structure-based selection of small molecules to alter allele-specific MHC class II antigen presentation. *J Immunol.* 2011;187(11):5921-30.

29. Chaparro RJ, and Dilorenzo TP. An update on the use of NOD mice to study autoimmune (Type 1) diabetes. *Expert Rev Clin Immunol.* 2010;6(6):939-55.

30. Lee KH, Wucherpfennig KW, and Wiley DC. Structure of a human insulin peptide-HLA-DQ8 complex and susceptibility to type 1 diabetes. *Nat Immunol.* 2001;2(6):501-7.

31. Eerligh P, van Lummel M, Zaldumbide A, Moustakas AK, Duinkerken G, Bondinas G, et al. Functional consequences of HLA-DQ8 homozygosity versus heterozygosity for islet autoimmunity in type 1 diabetes. *Genes Immun.* 2011;12(6):415-27.

32. Tollefsen S, Arentz-Hansen H, Fleckenstein B, Molberg O, Raki M, Kwok WW, et al. HLA-DQ2 and -DQ8 signatures of gluten T cell epitopes in celiac disease. *J Clin Invest.* 2006;116(8):2226-36.

33. Mah GT, Tejani AM, and Musini VM. Methyldopa for primary hypertension. *Cochrane Database Syst Rev.* 2009(4):Cd003893.

34. Broughton SE, Petersen J, Theodossis A, Scally SW, Loh KL, Thompson A, et al. Biased T cell receptor usage directed against human leukocyte antigen DQ8-restricted gliadin peptides is associated with celiac disease. *Immunity.* 2012;37(4):611-21.

35. Davis MM, Boniface JJ, Reich Z, Lyons D, Hampl J, Arden B, et al. Ligand recognition by alpha beta T cell receptors. *Annu Rev Immunol.* 1998;16:523-44.

36. Sjoerdsma A, Vendsalu A, and Engelman K. Studies on the metabolism and mechanism of action of methyldopa. *Circulation.* 1963;28:492-502.

37. Nakayama M, McDaniel K, Fitzgerald-Miller L, Kiekhaefer C, Snell-Bergeon JK, Davidson HW, et al. Regulatory vs. inflammatory cytokine T-cell responses to mutated insulin peptides in healthy and type 1 diabetic subjects. *Proc Natl Acad Sci U S A.* 2015;112(14):4429-34.

38. Yang J, Chow IT, Sosinowski T, Torres-Chinn N, Greenbaum CJ, James EA, et al. Autoreactive T cells specific for insulin B:11-23 recognize a low-affinity peptide register

in human subjects with autoimmune diabetes. *Proc Natl Acad Sci U S A.* 2014;111(41):14840-5.

39. James EA, Bui J, Berger D, Huston L, Roti M, and Kwok WW. Tetramer-guided epitope mapping reveals broad, individualized repertoires of tetanus toxin-specific CD4+ T cells and suggests HLA-based differences in epitope recognition. *Int Immunol.* 2007;19(11):1291-301.

40. Greenbaum CJ, Beam CA, Boulware D, Gitelman SE, Gottlieb PA, Herold KC, et al. Fall in C-peptide during first 2 years from diagnosis: evidence of at least two distinct phases from composite Type 1 Diabetes TrialNet data. *Diabetes.* 2012;61(8):2066-73.

41. Roep BO, and Peakman M. Antigen targets of type 1 diabetes autoimmunity. *Cold Spring Harb Perspect Med.* 2012;2(4):a007781.

42. Krogsgaard M, Prado N, Adams EJ, He XL, Chow DC, Wilson DB, et al. Evidence that structural rearrangements and/or flexibility during TCR binding can contribute to T cell activation. *Mol Cell.* 2003;12(6):1367-78.

43. Willcox BE, Gao GF, Wyer JR, Ladbury JE, Bell JI, Jakobsen BK, et al. TCR binding to peptide-MHC stabilizes a flexible recognition interface. *Immunity.* 1999;10(3):357-65.

44. Spanier JA, Sahli NL, Wilson JC, Martinov T, Dileepan T, Burrack AL, et al. Increased Effector Memory Insulin-Specific CD4+T-cells Correlate with Insulin Autoantibodies in Recent-Onset Type 1 Diabetic Patients. *Diabetes.* 2017; 66(12):3051-60.

45. Zhang L, Crawford F, Yu L, Michels A, Nakayama M, Davidson HW, et al. Monoclonal antibody blocking the recognition of an insulin peptide-MHC complex modulates type 1 diabetes. *Proc Natl Acad Sci U S A.* 2014;111(7):2656-61.

46. Dahan R, Gebe JA, Preisinger A, James EA, Tendler M, Nepom GT, et al. Antigen-specific immunomodulation for type 1 diabetes by novel recombinant antibodies directed against diabetes-associates auto-reactive T cell epitope. *J Autoimmun.* 2013;47:83-93.

47. Ostrov DA, Grant BJ, Pompeu YA, Sidney J, Harndahl M, Southwood S, et al. Drug hypersensitivity caused by alteration of the MHC-presented self-peptide repertoire. *Proc Natl Acad Sci U S A.* 2012;109(25):9959-64.

48. Illing PT, Vivian JP, Dudek NL, Kostenko L, Chen Z, Bharadwaj M, et al. Immune self-reactivity triggered by drug-modified HLA-peptide repertoire. *Nature.* 2012;486(7404):554-8.

49. White KD, Chung WH, Hung SI, Mallal S, and Phillips EJ. Evolving models of the immunopathogenesis of T cell-mediated drug allergy: The role of host, pathogens, and drug response. *J Allergy Clin Immunol.* 2015;136(2):219-34.

50. Pompeu YA, Stewart JD, Mallal S, Phillips E, Peters B, and Ostrov DA. The structural basis of HLA-associated drug hypersensitivity syndromes. *Immunol Rev.* 2012;250(1):158-66.

51. Klitz W, Maiers M, Spellman S, Baxter-Lowe LA, Schmeckpeper B, Williams TM, et al. New HLA haplotype frequency reference standards: high-resolution and large sample typing of HLA DR-DQ haplotypes in a sample of European Americans. *Tissue Antigens.* 2003;62(4):296-307.

52. Kitchen DB, Decornez H, Furr JR, and Bajorath J. Docking and scoring in virtual screening for drug discovery: methods and applications. *Nature reviews Drug discovery.* 2004;3(11):935-49.

53. Ferrara P, Gohlke H, Price DJ, Klebe G, and Brooks CL, 3rd. Assessing scoring functions for protein-ligand interactions. *J Med Chem.* 2004;47(12):3032-47.

54. Ewing TJ, Makino S, Skillman AG, and Kuntz ID. DOCK 4.0: search strategies for automated molecular docking of flexible molecule databases. *J Comput Aided Mol Des.* 2001;15(5):411-28.

55. Liu E, McDaniel K, Case S, Yu L, Gerhartz B, Ostermann N, et al. Exploring T cell reactivity to gliadin in young children with newly diagnosed celiac disease. *Autoimmune Dis.* 2014;2014:1-8.

56. Hennecke J, and Wiley DC. Structure of a complex of the human alpha/beta T cell receptor (TCR) HA1.7, influenza hemagglutinin peptide, and major histocompatibility complex class II molecule, HLA-DR4 (DRA*0101 and DRB1*0401): insight into TCR cross-restriction and alloreactivity. *J Exp Med.* 2002;195(5):571-81.

57. Sidney J, Southwood S, Moore C, Oseroff C, Pinilla C, Grey HM, et al. Measurement of MHC/peptide interactions by gel filtration or monoclonal antibody capture. *Curr Protoc Immunol.* 2013;Chapter 18:Unit 18.3.

58. Yu L, Eisenbarth G, Bonifacio E, Thomas J, Atkinson M, and Wasserfall C. The second murine autoantibody workshop: remarkable interlaboratory concordance for radiobinding assays to identify insulin autoantibodies in nonobese diabetic mice. *Ann N Y Acad Sci.* 2003;1005:1-12.

59. Yu L, Rewers M, Gianani R, Kawasaki E, Zhang Y, Verge C, et al. Antiislet autoantibodies usually develop sequentially rather than simultaneously. *J Clin Endocrinol Metab.* 1996;81(12):4264-7.

60. Rewers A, Babu S, Wang TB, Bugawan TL, Barriga K, Eisenbarth GS, et al. Ethnic differences in the associations between the HLA-DRB1*04 subtypes and type 1 diabetes. *Ann N Y Acad Sci.* 2003;1005:301-9.

61. Nagata M, Kotani R, Moriyama H, Yokono K, Roep BO, and Peakman M. Detection of autoreactive T cells in type 1 diabetes using coded autoantigens and an immunoglobulin-free cytokine ELISPOT assay: report from the fourth immunology of diabetes society T cell workshop. *Ann N Y Acad Sci.* 2004;1037:10-5.

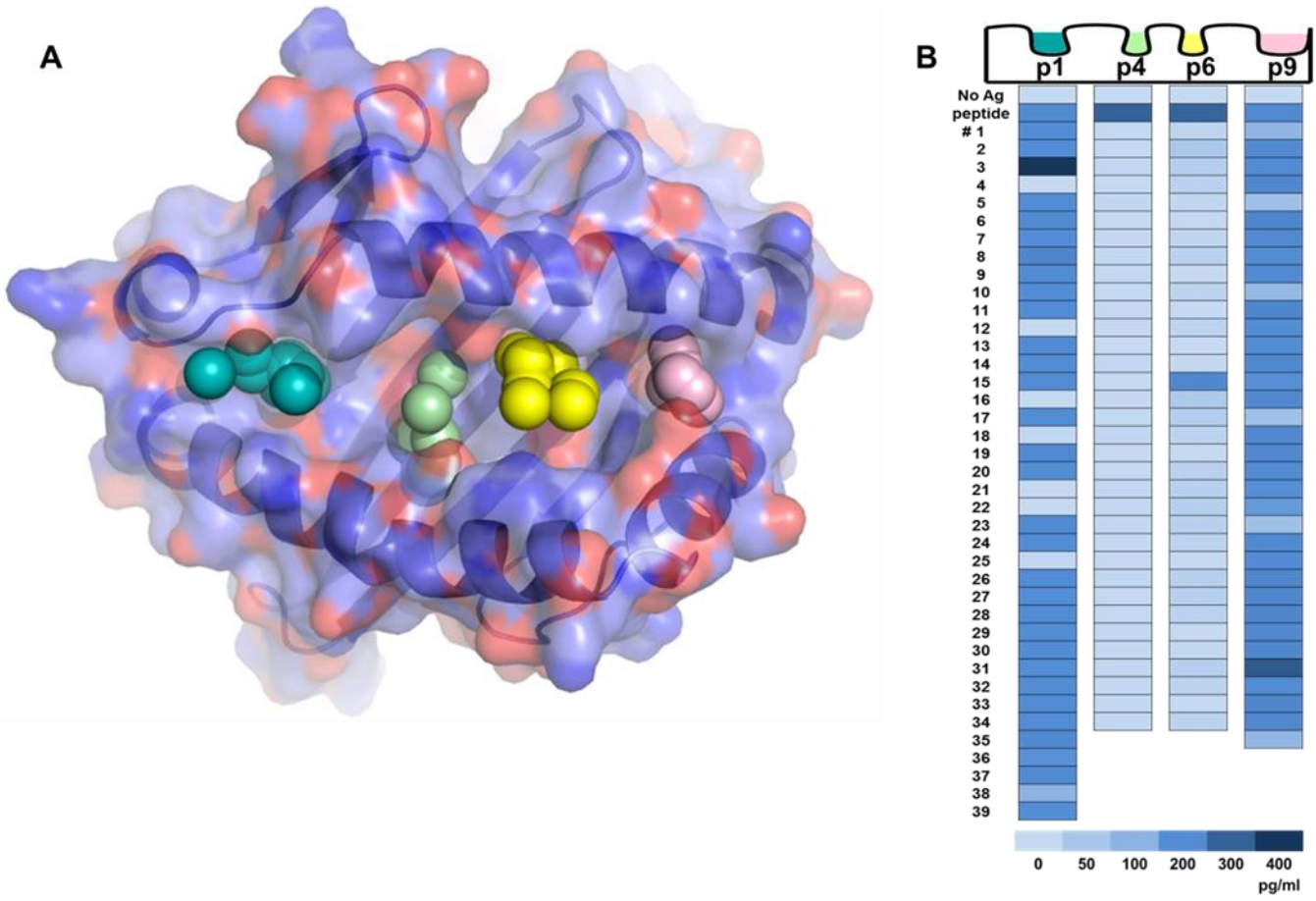

Figure 1. In silico screening of a small molecule library by molecular docking to structural pockets within the HLA-DQ8 peptide binding groove and in vitro screening of the top scoring compounds. (**A**) Molecular model of the DQ8 peptide binding cleft with pockets 1, 4, 6 and 9 depicted by colored spheres. Using a supercomputer, a repository of 139,735 compounds were docked into each pocket in 1000 different orientations and scored based upon the free energy of binding (ΔG). (**B**) The top scoring compounds were screened with an in vitro bioassay, which uses an immortalized T-cell that responds to an insulin epitope presented by DQ8. The T-cell receptor (TCR) α/β genes from an insulin B:9-23 restricted T-cell clone were retrovirally transduced into a T-cell line devoid of endogenous TCR to create a TCR transductant, named Clone 5. Clone 5 was cultured with insulin peptide plus small molecule in the presence of DQ8-transgenic murine splenocytes. After overnight culture, secreted IL-2 was measured in the cell culture supernatant

with a highly sensitive ELISA. In the heat map, no antigen (No Ag) is the response without in vitro added peptide and peptide represents response to peptide without an in vitro added small molecule. Numbers 1-39 depict tested compounds and all compounds were different for each pocket. The insulin B:9-23 peptide was used to screen pockets 1 and 9, while insulin B:13-23 was used to screen pockets 4 and 6 which resulted in a higher baseline IL-2 response. Supplemental Tables 1-4 lists the corresponding chemical structures, ΔG estimates from molecular docking, and rank based on overall free energy score.

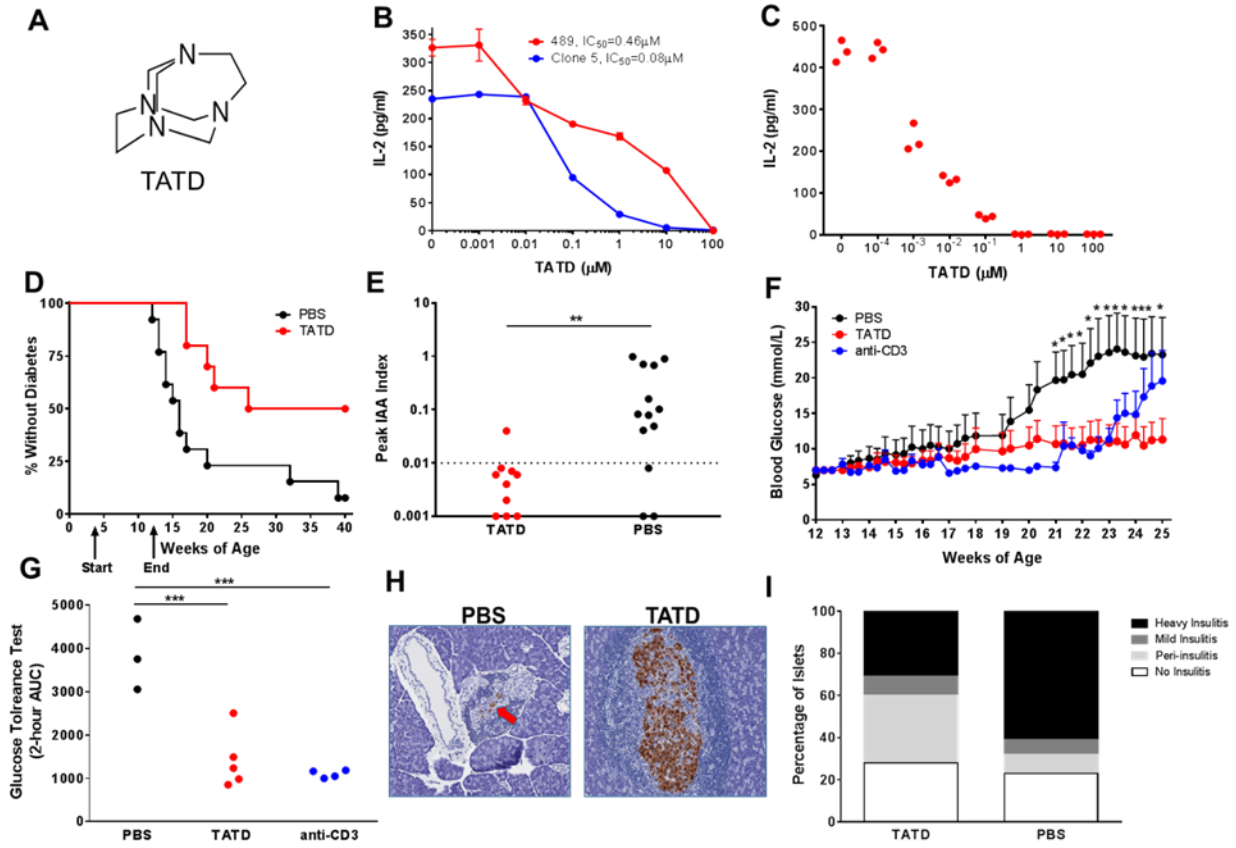

Figure 2. TATD blocks DQ8 restricted T-cell responses and prevents diabetes in NOD mice. (**A**) Chemical structure of TATD, 1,3,6,8-Tetraaza-tricyclo[4.4.1.1^{3,8}]dodecane. (**B**) TATD blocks an in vitro DQ8 restricted T-cell response to insulin B:13-23 (Clone 5) and deamidated α-gliadin$_{228-240}$ (489). Data shown as mean ± SEM and representative of 3 independent experiments. No antigen added to culture resulted in IL-2 levels < 3pg/ml. (**C**) TATD was cultured with recombinant α-gliadin/DQ8 protein and free peptide in conditions to allow peptide exchange. After washing, the recombinant protein was used to stimulate 489 with secreted IL-2 measured. Data are from triplicate wells and representative of 3 independent experiments; 489 in culture without protein resulted in IL-2 levels < 3pg/ml. (**D**) Female NOD mice were treated with TATD 20mg/kg (n=10) or PBS (n=13) by i.p. injection daily for 5 days each week from 4 to 12 weeks of age. p=0.006 using a Log-rank test. (**E**) Peak serum insulin autoantibody levels measured using a fluid-

phase RIA during the 40-week prevention study, **p=0.003 using a Mann-Whitney test; dotted line at 0.01 indicates a positive value. (**F**) Blood glucose levels during a late prevention study in which female NOD mice were treated with TATD 30mg/kg orally each day (n=9), 50ug of anti-CD3 mAb i.p. for 5 consecutive days (n=10), or PBS (n=10) beginning at 12 weeks of age and ending at 25 weeks. Data are depicted as mean ± SEM, *p<0.05 comparing TATD vs PBS using an ANOVA. (**G**) i.p. glucose tolerance test following cessation of study treatments, each dot represents an individual mouse. *** p<0.01 using a two-tailed unpaired t-test. (**H**) Representative pancreas section H&E stained from a PBS and TATD treated mouse, insulin staining in brown; images at 15X. (**I**) Insulitis scoring from at least 100 separate islets from TATD (n=3) and PBS (n=5) treated mice.

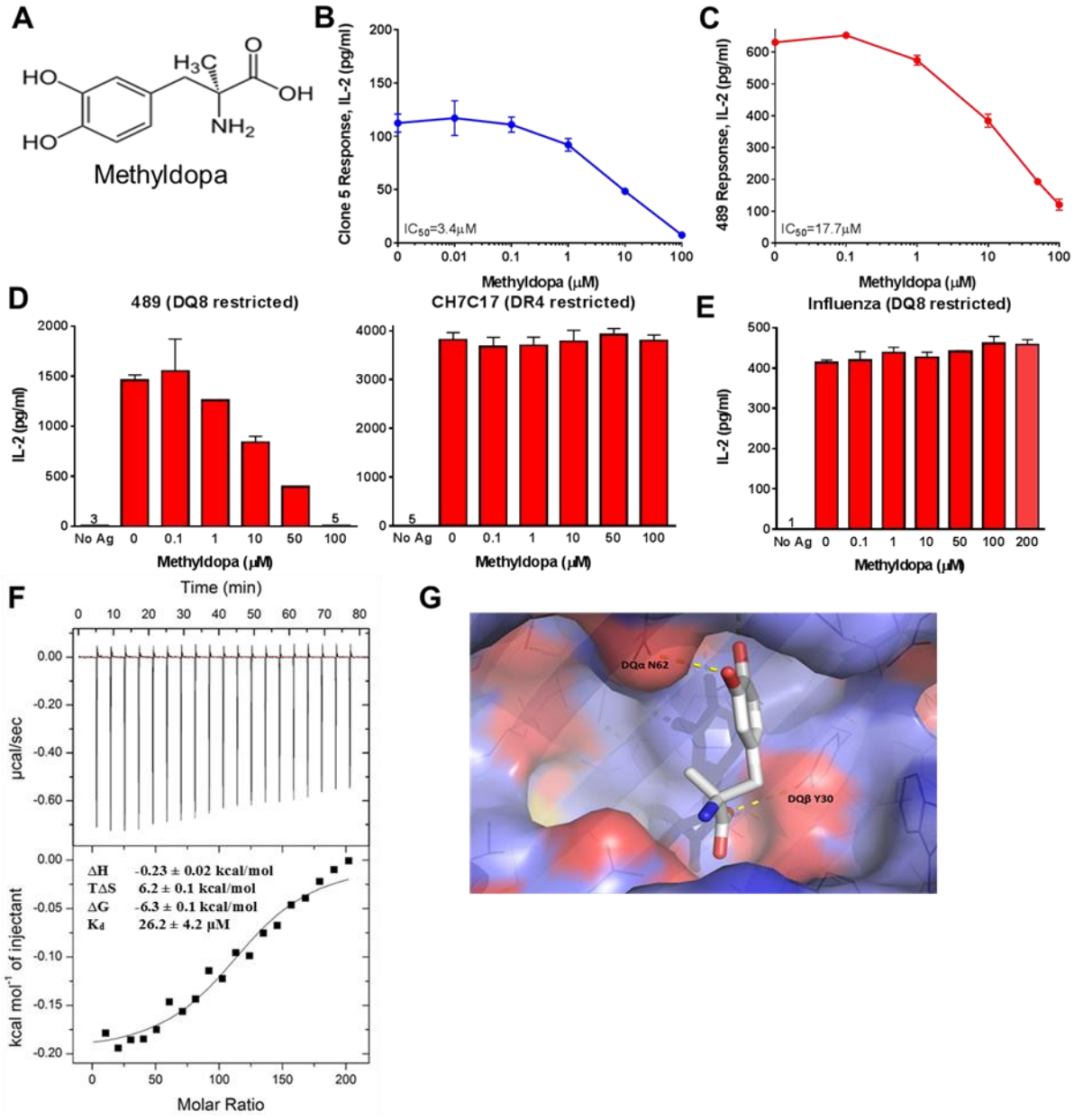

Figure 3. Methyldopa blocks DQ8 antigen presentation in vitro. (**A**) Methyldopa chemical structure. Methyldopa blocks an in vitro DQ8 restricted T-cell response to (**B**) Clone 5 responding to insulin B:13-23 and (**C**) 489 responding to deamidated α-gliadin presented by DQ8. The negative controls (no antigen added to culture) resulted in IL-2 levels < 3pg/ml. (**D**) Methyldopa specifically inhibits 489, a DQ8 restricted T-cell response while not altering C7CH17, a DR4 restricted T-cell response to the hemagglutinin peptide, $HA_{306-318}$. An EBV transformed B-cell line

homozygous for DQ8 and DR4 was used as APCs in this experiment, such that each APC had DQ8 and DR4 on the cell surface. (**E**) Methyldopa does not inhibit a DQ8 restricted T-cell response to an influenza peptide, $HA_{102-118}$. Data are shown as mean ± SEM and representative of 3 independent experiments in **B-E**. (**F**) Representative isothermal titration calorimetry data titrating methyldopa into DQ8 protein. Top panel shows heat released as a function of time from 2µl injections of 4mM methyldopa titrated into the sample cell containing 4µM of DQ8 protein at 25ºC. The lower panel depicts the fitted binding curve along with the measured thermodynamic parameters and calculated dissociation constant (K_D) from 3 independent experiments reported as mean ± SEM. (**G**) Molecular docking model of methyldopa in the DQ8 antigen-binding cleft shows potential H bonds: between a methyldopa hydroxyl group and DQα62 asparagine on the DQα-helix and between the methyldopa carboxylic acid and DQβ30 tyrosine on the floor of the cleft.

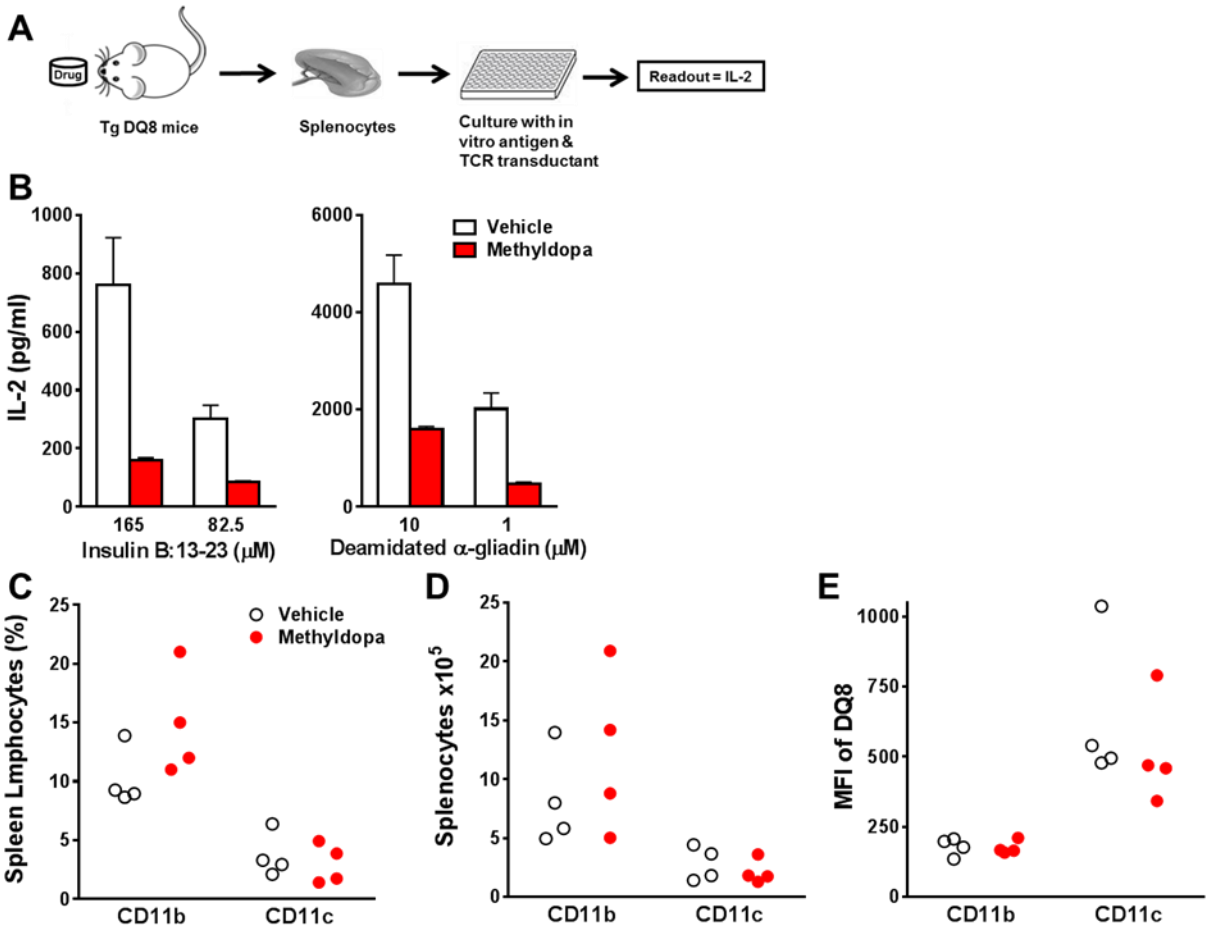

Figure 4. Methyldopa blocks DQ8 antigen presentation in vivo. (**A**) Diagram of the assay used to monitor the potency of methyldopa to block DQ8 in transgenic mice. (**B**) Adult DQ8-tansgenic mice were gavaged with vehicle or 200mg/kg methyldopa three times daily for four days (n=4 per group). Ex vivo splenocytes were used as APCs to present different concentrations of the insulin B:13-23 peptide or a deamidated α-gliadin peptide to Clone 5 or 489, respectively. No methyldopa was added to the in vitro culture. 200mg/kg is equivalent to 1000mg three times daily in a 60kg human. Bar graphs represent mean ± SEM, representative of 3 independent experiments. (**C**) Percentages and (**D**) numbers of $CD11b^+$ and $CD11c^+$ cells in the spleens of treated mice. (**E**) Mean fluorescent intensity of DQ8 cell surface staining on each population. Each dot represents and individual mouse.

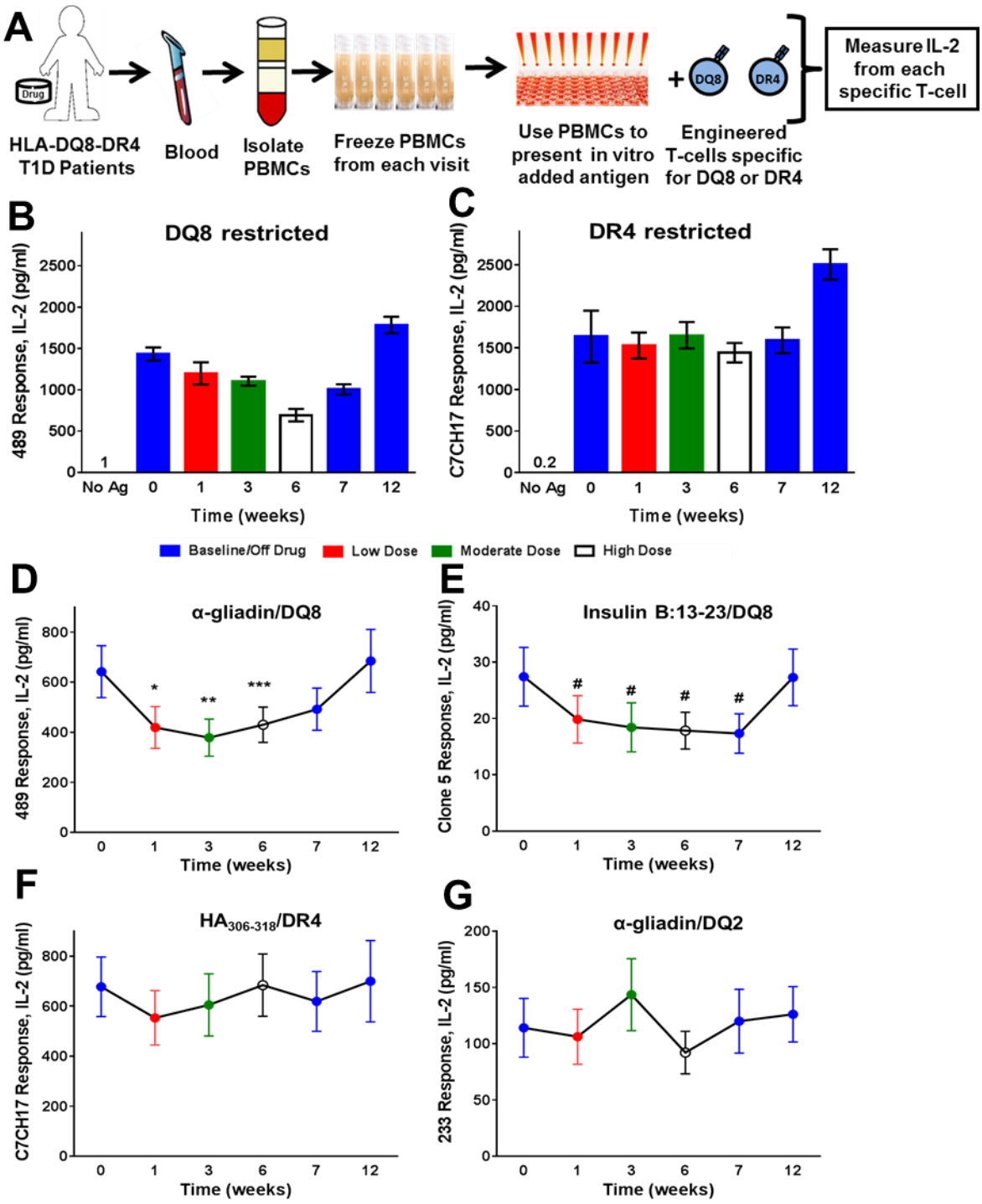

Figure 5. Methyldopa treatment specifically blocks DQ8 antigen presentation in recent-onset type 1 diabetes patients with the DQ8 allele. (**A**) Diagram of assay used to monitor specific MHC class II antigen presentation. Peripheral blood mononuclear cells (PBMCs) were isolated

and frozen from each study visit. These primary PBMCs were then thawed and used as antigen presenting cells to stimulate engineered T-cells, TCR transductants, responding to a specific peptide presented by a given MHC class II molecule (DQ8, DR4 or DQ2). Secreted IL-2 from each TCR transductant was measured by a highly sensitive ELISA. (**B**) An individual study subject response for 489 (DQ8 restricted) and (**C**) C7CH17 (DR4 restricted). Data are shown as mean ± SEM from triplicate wells at each time point during the study. Colors represent time on and off drug; participants underwent a dose titration with a low dose (500mg twice daily), moderate dose (500mg three time daily), high dose (2-3 grams divided daily) and then off drug. No Ag = no in vitro added antigen to the assay. (**D**) Summative data from study participants (n=20) for response to 489 and (**E**) Clone 5, both DQ8 restricted. *p=0.001, **p<0.001, ***p=0.02, #p<0.01 using a longitudinal mixed-effects model that compares the least-squares mean at each time point to baseline. (**F**) Data from study participants with DR4 subtypes (n=18) able to present and stimulate the $HA_{306-318}$ restricted TCR transductant (C7CH17). (**G**) Response to a DQ2 TCR transductant (233 responding to α-$gliadin_{62-73}$) over the study duration in subjects with a DQ2 allele (n=7). The negative control (no antigen added to culture) resulted in IL-2 levels < 2pg/ml for each subject and individual TCR transductants. Data in **D-G** are depicted as least-squares means ± standard error for the study cohort; individual responses are shown in Supplemental Figure 10.

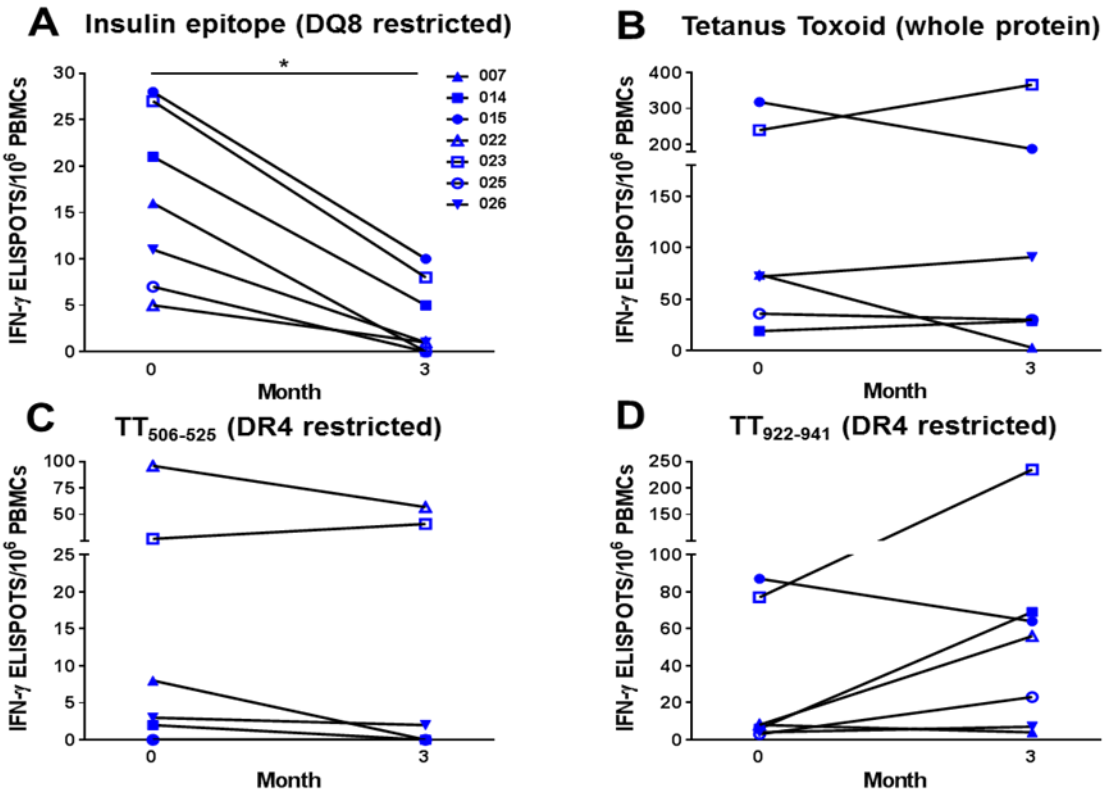

Figure 6. Methyldopa treatment reduces primary antigen-specific T cells restricted to HLA-DQ8 but not those presented by DR4. Cryopreserved peripheral blood mononuclear cells were thawed, cultured in the presence or absence of protein/peptide for 48 hours, washed, and then transferred to an IFN-γ monoclonal antibody-coated plate for overnight culture, followed by development and enumeration of ELISPOTs. Depicted are IFN-γ ELISPOT results from study subjects to (**A**) an insulin B chain mimotope, B:9-23 (B22E), known to be presented by DQ8 (**B**) whole tetanus toxin (TT) protein (**C**) an epitope of TT consisting of amino acids 506-525 known to be presented by DR4 and (**D**) another DR4 restricted TT epitope, amino acids 922-941. Seven study subjects responded to the insulin B chain mimotope at baseline and were further evaluated for responses to TT protein and epitopes. Each data point represents the total spot number for a given condition from triplicate wells minus the total spot number without antigen (background) for an individual. Symbols represent the same individual tested for each condition. *p=0.016 using

the Wilcoxon matched-pairs signed rank test, p = NS for TT, $TT_{506-525}$ and $TT_{922-941}$. ELISPOT counts for each individual and condition, including no antigen as a negative control and whole TT as a positive control, at baseline and 3 months is in Supplemental Table 8.

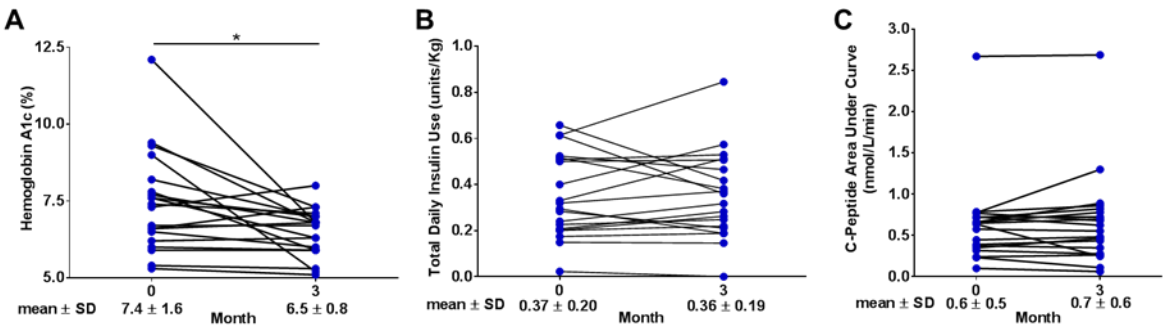

Figure 7. Measures of glycemic control and beta cell function among study participants. Individual responses show (**A**) an improvement in hemoglobin A1c, a measure of average blood glucose over the preceding 3 months, from baseline to study completion. *p=0.008 using the Wilcoxon matched-pairs signed rank test. (**B**) Similar exogenous insulin use/Kg body weight from beginning to end of the study. (**C**) Maintenance of beta cell function, as measured by the C-peptide 2 hour AUC following a mixed meal tolerance test, compared to baseline levels. C-peptide is a measure of endogenous insulin secretion as both are secreted in a 1:1 molar ratio. Individuals ingested a liquid meal (Boost) with a fixed amount of protein, fat and carbohydrate in the fasting state followed by the timed measurements of serum C-peptide at 0, 15, 30, 60, 90 and 120 minutes to compute the AUC. Each data point represents a single individual with a line connecting the same study participant; n=20 subjects in **A-C** with mean ± SD reported for the entire cohort at the start of study and completion.

Table 1. Methyldopa Structure Activity Relationships

Compound*	**Clone 5 IC_{50} (insulin/DQ8)**	**489 IC_{50} (α-gliadin/DQ8)**
α-methyldopa	3.4 μM	17.7 μM
α-methylphenylalanine	No inhibition	No inhibition
α-methyltyrosine	No inhibition	No inhibition
3-O-methyl methyldopa	No inhibition	No inhibition
α-methyldopa ethyl ester	5.8 μM	7.8 μM
α-methylnorepinephrine	No Inhibition	No inhibition

*Compound structures depicted in Supplemental Table 6.

Table 2. Clinical characteristics of study subjects receiving methyldopa (n=20).

Age, years	
Median	22
Mean (SD)	24.8 (7.6)
Range	18-43
T1D Duration, days	
Median	90
Mean (SD)	133 (143.3)
Range	21-566
Sex, number (%)	
Male	13 (65)
Female	7 (35)
Ethnicity, number (%)	
Caucasian	17 (85)
African American	2 (10)
Hispanic	1 (5)
Islet autoantibody positive*, number (%)	
One	7 (35)
Two	5 (25)
Three	8 (40)
Four	0 (0)
HLA-DQ genotype, number (%)	
One DQ8 allele	16 (80)
Two DQ8 alleles	4 (20)

*Insulin autoantibodies only included if measured within 21 days of starting exogenous insulin.